

## Surface three-body recombination in spin-polarized atomic hydrogen

L. Philip H. de Goeij, Henk T. C. Stoof, J. M. Vianney A. Koelman, and Boudewijn J. Verhaar  
*Department of Physics, Eindhoven University of Technology, 5600 MB Eindhoven, The Netherlands*

Jook T. M. Walraven

*Natuurkundig Laboratorium der Universiteit van Amsterdam, 1018XE Amsterdam, The Netherlands*

(Received 9 June 1987; revised manuscript received 4 April 1988)

We determine the rate of  $b + b + b$  surface dipole recombination for hydrogen atoms adsorbed on a  $^4\text{He}$  film. The calculation is based on the Kagan mechanism adapted to a  $2\frac{1}{2}$ -dimensional initial state. We find a rate constant  $L_s^{\text{eff}} = 2.7(7) \times 10^{-25} \text{ cm}^4 \text{ s}^{-1}$  at  $B = 7.6 \text{ T}$  and  $T = 0.4 \text{ K}$ , which is roughly a factor of 6 smaller than the experimental results. The magnetic-field dependence also disagrees with experiment. A scaling approach, although leading to the correct order of magnitude, is discussed and shown to be unsatisfactory. The reliability of some of our approximations is estimated. We conclude that the dipole-exchange mechanism is probably responsible for the discrepancies with experiment.

### I. INTRODUCTION

Since the pioneering work of London<sup>1</sup> in the early sixties, the phenomena of superconductivity in metals and superfluidity in liquid  $^4\text{He}$  have been believed to be manifestations of quantum mechanics on a macroscopic scale. Since then superfluidity has been observed in liquid  $^3\text{He}$  and in the lower part of the energy spectrum of atomic nuclei. It is also believed to play a role in neutron stars. The prospect of observing quantum phenomena on a macroscopic scale in electron-spin polarized atomic hydrogen  $\text{H}_\downarrow$  has strongly stimulated the investigation of this gas at low temperatures ( $T = 80 \text{ mK} - 1 \text{ K}$ ) in liquid-helium-covered sample cells.<sup>2,3</sup> Compared with the above-mentioned systems, an attractive feature of  $\text{H}_\downarrow$  is the possibility of observing Bose-Einstein condensation in a wide range of controllable circumstances of temperature and density. Up to now the decay of the gas into  $\text{H}_2$  molecules has been the major obstacle to reaching the density-temperature regime of interest.

Polarizing the electron spins in a strong magnetic field ( $B \approx 10 \text{ T}$ ) strongly reduces the decay and densities in the range  $n = 10^{16} - 10^{17} \text{ cm}^{-3}$  were achieved. The next step towards Bose-Einstein condensation was the creation of a doubly polarized  $\text{H}_{\downarrow\uparrow}$  gas, where both the electron and proton spins are polarized. The double polarization is achieved by the spontaneous selective recombination<sup>4</sup> of the hyperfine  $a$ -state population as a result of the small admixture of the antiparallel electron-spin state (the  $1s$  hyperfine levels of atomic H are as usually labeled  $a, b, c, d$  in order of increasing energy).

The first experiments based on this mechanism still showed a slow decay, which was interpreted for low temperatures in terms of  $b \rightarrow a$  surface relaxation, studied theoretically in Refs. 5–9, followed by rapid recombination. In Ref. 8 it was first pointed out that this interpretation led to a discrepancy of order 50 between experimental and theoretical values for the  $b \rightarrow a$  surface relax-

ation constant  $G_s$ . Many attempts were made to resolve this discrepancy, in particular via a three-dimensional calculation of the collision of adsorbed atoms<sup>9</sup> and a possible role of surface dimers.<sup>9,10</sup>

Further experimental progress took place by compression<sup>2,3</sup> of  $\text{H}_{\downarrow\uparrow}$  to densities up to  $4.5 \times 10^{18} \text{ cm}^{-3}$ . This is to be compared with the critical density for the transition to the Bose-Einstein condensed phase, predicted for an ideal gas at

$$n_c = (m_H k_B T_c / 3.31 \hbar^2)^{3/2} \approx 1.6 \times 10^{19} \text{ cm}^{-3}$$

for  $T_c = 100 \text{ mK}$ . The main obstacle to achieving higher densities now turned out to be a process of magnetic-dipole induced recombination in a three-body collision of  $b$  atoms, first described by Kagan, Vartan'yants, and Shlyapnikov.<sup>11</sup> Hess *et al.*<sup>12</sup> first noticed that this same process taking place at the surface could have been responsible for the apparent discrepancy at lower densities. A reanalysis of previous experiments and a new experiment by Reynolds *et al.*<sup>13</sup> confirmed this and showed  $G_s$  to agree with theory taking into account the roughness of the cell walls.

With respect to the three-body rate constant  $L$  the situation is less satisfactory. For the bulk constant the magnitude is roughly in agreement with Kagan's calculation for  $B = 7.8 \text{ T}$ . The field dependence, however, shows a disagreement. At the temperature relevant for achieving Bose-Einstein condensation, the Kagan process takes place primarily at the surface. The present paper deals with the theory of this surface process. The main results were published earlier as a short report<sup>14</sup> (further referred to as I), with only a superficial description of the methods used and without a physical interpretation of the results.

The decay of  $\text{H}_{\downarrow\uparrow}$  through the three-body channel is described by an additional  $n^3$  term in the rate equation

$$\frac{dn}{dt} = -G^{\text{eff}} n^2 - L^{\text{eff}} n^3. \quad (1)$$

Like the two-body relaxation constant,  $L^{\text{eff}}$  is the sum of bulk and surface contributions

$$L^{\text{eff}} = L_g^{\text{eff}} + L_s^{\text{eff}} \left[ \frac{A}{V} \lambda_{\text{th}}^3(T) \exp(-3\epsilon_0/kT) \right]. \quad (2)$$

Here,  $A/V$  is the surface-to-volume ratio,  $\lambda_{\text{th}}$  the thermal de Broglie wavelength, and  $-\epsilon_0$  the adsorption energy. It should be noted that the  $L_{g,s}^{\text{eff}}$  constants include a subsequent recombination of the final H atom in case its electron spin is flipped:

$$L_{g,s}^{\text{eff}} = L_{g,s}^{-1/2} + 2L_{g,s}^{+1/2}, \quad (3)$$

the superscripts  $\pm 1/2$  standing for the spin-projection  $m_{s_3}$  of this atom along  $\mathbf{B}$ . The constants  $L_{g,s}^{-1/2}$  and  $L_{g,s}^{+1/2}$  denote the pure single- and double-spin-flip contributions to  $L_{g,s}^{\text{eff}}$ . In this paper we shall sometimes consider the rate constants

$$L_{g,s} = L_{g,s}^{-1/2} + L_{g,s}^{+1/2}, \quad (4)$$

representing the pure  $b + b + b \rightarrow \text{H}_2 + \text{H}$  recombination decay. For comparison with experiment, however, we present results of the separate contributions  $L_s^{\pm 1/2}$ , as well as the total effective rate constant  $L_s^{\text{eff}}$ . A weight factor close to 2 for the double-spin-flip contribution has been considered in several experimental papers. Results to be presented here allow the derivation of  $L_s^{\text{eff}}$  for such weight factors.

In this paper we reexamine the results of I with respect to the surface rate constant  $L_s^{\text{eff}}$ . Throughout this paper we approximate the helium film as an inert surface, the

effect of which on an H atom is represented by a potential well  $V(z)$ . In Sec. II we present expressions for  $L_s^{\pm 1/2}$  in terms of three-body collision amplitudes. In addition we review our method to calculate  $L_s^{\pm 1/2}$ . In Sec. III we describe our results. It turns out that they show some difference with I, primarily by the use of an H-H singlet potential, describing more accurately the H-H binding energy data. A major discrepancy still exists with experimental data, both with respect to absolute magnitude and field dependence. In Sec. IV we confront our method with the scaling procedure, described by Kagan *et al.*<sup>15</sup> We show that the scaling method is unsatisfactory, although the results do agree roughly with experiment (as to magnitude, not to field dependence) and although it enables one to obtain an  $L_s^{\text{eff}}$  value without cumbersome calculations. One of our model assumptions in Secs. II and III is the complete neglect of the influence of the helium surface on the final  $\text{H}_2 + \text{H}$  state. In I we already pointed out briefly that some of the effects which arise when this assumption is relaxed are estimated to be small. In Sec. V we describe how the estimate is carried out and present its results. Some conclusions of the present paper are given in Sec. VI.

## II. CALCULATION OF $L_s^{\pm 1/2}$

Past experience in connection with two-body rates<sup>5-9</sup> shows that factor of 2 errors easily arise from a careless treatment of identical-particle aspects. Since a corresponding factor of 6 in the case of three H atoms is of the same order of magnitude as the final discrepancy with experiment, it is of importance to specify in sufficient detail the rate expression which is used as a starting point.

We start from the expression<sup>16</sup>

$$L_s^{\pm 1/2} = (2\pi\hbar)^7 \frac{1}{4m_H} \left\langle \sum_n \int dP_Z \int d\hat{q}_f q_f |f_{q_f P_Z n \pm 1/2, \mathbf{p}_i, \mathbf{q}_i}|^2 \right\rangle_{\text{thermal}} \quad (5)$$

with the scattering amplitude  $f$  being given by

$$f_{q_f P_Z n \pm 1/2, \mathbf{p}_i, \mathbf{q}_i} = \frac{\frac{2}{3}m_H}{2\pi\hbar^2} \left\langle \psi^{(-)}(\mathbf{q}_f P_Z n \pm \frac{1}{2}) \left| V_d \sum_P P \right| \psi^{(+)}(\mathbf{p}_i, \mathbf{q}_i) \right\rangle. \quad (6)$$

The operator  $V_d$  is the sum of magnetic dipole interactions, while  $\psi^{(+)}$  and  $\psi^{(-)}$  are the initial and final three-atom states, including the central (singlet and triplet) interactions. By  $\mathbf{p}_i$  and  $\mathbf{q}_i$  we indicate a combination of two-dimensional (2D) Jacobi relative momentum vectors,<sup>17</sup> which together with the bound  $z$  states of the atom define the plane-wave part of  $\psi^{(+)}$ . The initial spin state ( $M_S = -\frac{3}{2}$ ) is suppressed in our notation. For the sake of definiteness we choose  $\mathbf{p}_i$  to be the momentum of atom 1 relative to 2, while  $\mathbf{q}_i$  is the momentum of atom 3 relative to the center-of-mass of atoms 1 and 2. The label  $n$  denotes a particular molecular state of atoms 1 and 2. For phase-space reasons we neglect the possibility that a final atom is again adsorbed to the surface. The plane-wave part of the final state  $\psi^{(-)}$  is a state in which an atom and a molecule with relative 3D momentum  $\mathbf{q}_f$  collide with a wall with total perpendicular momentum  $P_Z$ .

The normalization of the states  $\psi^{(+)}$  and  $\psi^{(-)}$  is chosen according to

$$\begin{aligned} \langle \psi^{(+)}(\mathbf{p}'_i, \mathbf{q}'_i) | \psi^{(+)}(\mathbf{p}_i, \mathbf{q}_i) \rangle &= \delta(\mathbf{p}'_i - \mathbf{p}_i) \delta(\mathbf{q}'_i - \mathbf{q}_i), \\ \langle \psi^{(-)}(P'_Z, \mathbf{q}'_f, n', m'_s) | \psi^{(-)}(P_Z, \mathbf{q}_f, n, m_s) \rangle & \\ &= \delta(P'_Z - P_Z) \delta(\mathbf{q}'_f - \mathbf{q}_f) \delta_{n'n} \delta_{m'_s m_s}. \end{aligned} \quad (7)$$

The model that we use to evaluate Eq. (5) is based on the Kagan dipole mechanism.<sup>11</sup> In this description of the recombination the electronic dipolar interactions induce a transition from a  $b + b + b$  incoming state to a final state, consisting of a bound pair of atoms (1 and 2) and atom 3, which does not interact with this pair. In view of this and the selection rule  $S_{12} = 1 \rightarrow S_{12} = 1$ , the dipolar interaction between 1 and 2 does not contribute. It was pointed out in Ref. 18 that such a contribution does arise

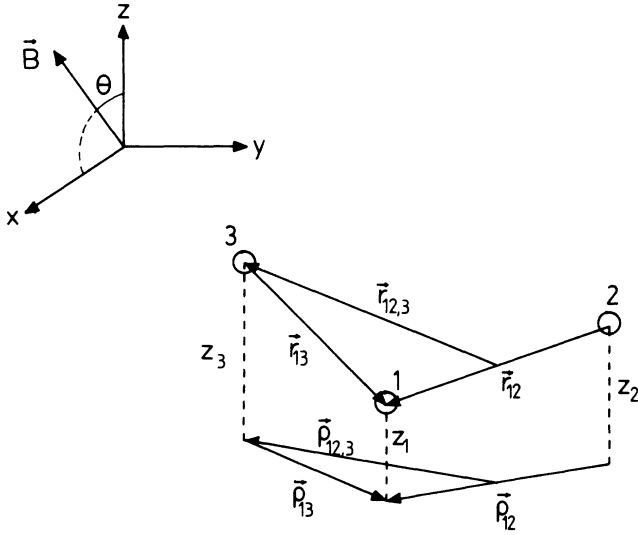


FIG. 1. Situation for three-body collisions on a  $^4\text{He}$  film. The distance of particle  $i$  from the surface is denoted by  $z_i$ . Furthermore,  $\mathbf{r}_{ij}, \mathbf{r}_{ij,k}$  and  $\boldsymbol{\rho}_{ij}, \boldsymbol{\rho}_{ij,k}$  are 3D and 2D Jacobi momenta, and  $\theta$  is the angle between magnetic-field direction and surface normal.

when an additional exchange interaction of particle 3 with 1 or 2 in the final state is taken into account. This dipole-exchange mechanism and possible other more complicated higher-order processes are neglected in the present paper. As for now the inclusion of this mechanism in surface calculations is not feasible.

Figure 1 shows the geometry of the system. We use Jacobi coordinates  $\mathbf{r}_{ij}, \mathbf{r}_{ij,k}$  and their projections  $\boldsymbol{\rho}_{ij}, \boldsymbol{\rho}_{ij,k}$  on the surface. To calculate  $f$ , we first consider the initial state  $|\psi^{(+)}(\mathbf{p}_i \mathbf{q}_i)\rangle$  of Eq. (6). This represents a state

$$\sum_P Pu \rightarrow \bar{u}(\boldsymbol{\rho}_{12}, \boldsymbol{\rho}_{13}) = [v_{\mathbf{k}'_{12}}^t(\boldsymbol{\rho}_{12}) + v_{-\mathbf{k}'_{12} - \mathbf{k}'_{13}}^t(\boldsymbol{\rho}_{12})] v_{\mathbf{k}'_{13}}^t(\boldsymbol{\rho}_{13}) + [v_{\mathbf{k}'_{13}}^t(\boldsymbol{\rho}_{12}) + v_{-\mathbf{k}'_{12} - \mathbf{k}'_{13}}^t(\boldsymbol{\rho}_{12})] v_{\mathbf{k}'_{12}}^t(\boldsymbol{\rho}_{13}) \\ + [v_{\mathbf{k}'_{12}}^t(\boldsymbol{\rho}_{12}) + v_{\mathbf{k}'_{13}}^t(\boldsymbol{\rho}_{12})] v_{-\mathbf{k}'_{12} - \mathbf{k}'_{13}}^t(\boldsymbol{\rho}_{13}), \quad (10)$$

in which  $\mathbf{k}'_{12} = (\mathbf{p}_i + \frac{1}{2}\mathbf{q}_i)/\hbar$ ,  $\mathbf{k}'_{13} = -\mathbf{q}_i/\hbar$ . Furthermore, the 2D two-particle relative wavefunction  $v_{\mathbf{k}}^t(\boldsymbol{\rho})$  has  $\exp(i\mathbf{k} \cdot \boldsymbol{\rho})/(2\pi\hbar)$  as a plane-wave part. Note that this Kagan-like replacement destroys partly the symmetry of  $\sum_P Pu$ . Note furthermore that the combination of six terms in Eq. (10) describes correctly the asymptotic plane-wave part.

In the volume case the six terms are identical in the  $T=0$  limit, leading to Kagan's results. We believe that Eq. (10) is a reasonable approximation, since the volume of configuration space in which particles 2 and 3 are closely together and thus correlated is only a small fraction of the total volume contributing significantly to the dipole integral. For low temperatures the only significant contribution of  $v_{\mathbf{k}}^t(\boldsymbol{\rho})$  to the amplitude comes from the lowest partial wave  $m=0$ , which for low  $k$  separates further into  $\rho$ - and  $k$ -dependent factors:<sup>20</sup>

of three noninteracting H atoms bound to the surface, i.e.,

$$|\mathbf{p}_i \mathbf{q}_i\rangle \doteq \phi_0(z_1)\phi_0(z_2)\phi_0(z_3) \left[ \frac{e^{i(\mathbf{p}_i \boldsymbol{\rho}_{12} + \mathbf{q}_i \boldsymbol{\rho}_{12,3})/\hbar}}{(2\pi\hbar)^2} \right] \\ \times \chi_{S=3/2, M_S=-3/2}(1, 2, 3), \quad (8)$$

of which the spatial part is distorted by the mutual triplet interactions. For this distortion we use the “ $2\frac{1}{2}$  dimensional” model,<sup>8,9</sup> which has proved to be very successful for the description of two-particle collisions along the surface. In this model the distortion affects only the factor between large parentheses in Eq. (8). It is replaced by a solution  $u(\boldsymbol{\rho}_{12}, \boldsymbol{\rho}_{12,3})$  of the two-dimensional Schrödinger equation for three H atoms mutually interacting by means of triplet potentials  $V_i$  averaged over the  $z$  motion of the atoms:

$$V^{\text{eff}}(\boldsymbol{\rho}_{ij}) = \int_{-\infty}^{\infty} dz_i \int_{-\infty}^{\infty} dz_j \phi_0^*(z_i)\phi_0^*(z_j) \\ \times V_i(r_{ij})\phi_0(z_i)\phi_0(z_j). \quad (9)$$

In the spin part  $\chi$  of Eq. (8) the magnetic quantum number refers to the magnetic-field direction.

The calculation of  $u(\boldsymbol{\rho}_{12}, \boldsymbol{\rho}_{12,3})$  is a two-dimensional three-atom problem. It could be obtained with the help of the Faddeev formalism<sup>18,19</sup> in two dimensions. Instead of this, however, we follow the method of Kagan *et al.*<sup>11</sup> We approximate  $u(\boldsymbol{\rho}_{12}, \boldsymbol{\rho}_{12,3})$  by only taking into account spatial correlations between the atoms of the recombining pair (1 and 2) and the pair (1-3 or 2-3) interacting via the dipolar interaction. We start with the symmetrized free state and replace the exponentials of the recombining pair and dipole pair by two-particle triplet scattering states. For instance, for the  $V_d(1,3)$  term of Eq. (6) we make the replacement

$$v_{\mathbf{k}}^t(\boldsymbol{\rho}) \simeq g(k)\hat{v}^t(\boldsymbol{\rho}), \quad (11)$$

with

$$g(k) = \frac{-1}{\left[ \frac{\pi^2}{4} + [\gamma + \ln(ka/2)]^2 \right]^{1/2}} \quad (12)$$

and

$$\hat{v}^t(\boldsymbol{\rho}) = \frac{\ln(\rho/a)}{2\pi\hbar} \quad (13)$$

just outside the potential range. Here,  $\gamma$  is Euler's constant and  $a$  is the 2D scattering length, which for the potential given by Eq. (9) has the value of  $2.4a_0$ , if the Mantz-Edwards wave function<sup>21</sup> is chosen for  $\phi_0(z)$ . Note that  $v_{\mathbf{k}}^t(\boldsymbol{\rho})$  differs in normalization from the radial wave function in Ref. 21. A  $T=0$  calculation, as for

volume recombination, is now impossible, because of the logarithmic  $k$  dependence in Eq. (12). These equations, however, still enable us to derive a low- $T$  approximation, since the energy dependence is now contained in a separate factor. We will use this later to calculate the thermally averaged quantity  $L_s^{\pm 1/2}$ .

We now turn to the final state  $|\psi^{(-)}(\mathbf{q}_f P_Z n \pm \frac{1}{2})\rangle$  of Eq. (6). In the previous section we defined it as an eigenstate of the Hamiltonian with central interactions between the atoms and atom-wall, molecule-wall interactions included. We now follow Kagan, however, in leaving out the atom-molecule interaction. Furthermore, in view of the rather high  $\text{H} + \text{H}_2$  relative kinetic energy ( $\sim 60$  K for  $B = 10$  T,  $v = 14$ ,  $j = 3$  and  $m_{s_3} = -\frac{1}{2}$ ), we neglect the attractive part of the surface potential ( $\sim 4.5$  K) and replace it by a perfectly reflecting rigid wall. As a first step, however, we will leave out the wall completely. An estimate of the effects neglected with this approxima-

tion is given in Sec. V.

On the basis of this the final state reduces to

$$\begin{aligned} |\psi^{(-)}(\mathbf{q}_f P_Z n m_{s_3})\rangle &\hat{=} u_{vjm}(\mathbf{r}_{12}) \frac{e^{iP_Z Z/\hbar}}{(2\pi\hbar)^{1/2}} \\ &\times \frac{e^{i\mathbf{q}_f \cdot \mathbf{r}_{12,3}/\hbar}}{(2\pi\hbar)^{3/2}} \chi_{S_{12}=0, M_{S_{12}}=0}(1,2) \\ &\times \chi_{1/2, m_{s_3}}(3). \end{aligned} \quad (14)$$

In Eq. (14)  $Z$  is the center-of-mass position perpendicular to the surface and  $u_{vjm}$  is the molecular wave function ( $m$  relative to  $z$ ). It turns out that only odd  $j$  final states are possible, since the  $V_d(1,3)$  and  $V_d(2,3)$  terms of  $f$  cancel for even  $j$  and are equal for odd  $j$ . Using Eqs. (8), (10), and (14) we obtain for the amplitude

$$\begin{aligned} f &= \frac{\frac{2}{3}m_H}{2\pi\hbar^2} \frac{2\delta_{j,\text{odd}}}{(2\pi\hbar)^2} \int dZ \int d\mathbf{r}_{12} \int d\mathbf{r}_{13} e^{-i\mathbf{q}_f \cdot (\mathbf{r}_{12}/2 - \mathbf{r}_{13})/\hbar} e^{-iP_Z Z/\hbar} u_{vjm}^*(\mathbf{r}_{12}) \\ &\times \langle \chi_{S_{12}=0, M_{S_{12}}=0}(1,2) \chi_{1/2, m_{s_3}}(3) | V_d(1,3) | \chi_{S=3/2, M_S=-3/2}(1,2,3) \rangle \\ &\times \bar{u}(\boldsymbol{\rho}_{12}, \boldsymbol{\rho}_{13}) \phi_0(z_1) \phi_0(z_2) \phi_0(z_3). \end{aligned} \quad (15)$$

To evaluate the integrals it is convenient to use cylindrical coordinates with the surface normal as a symmetry axis. The dipolar interaction can be written as a scalar product of rank-two tensor operators  $\Sigma^{(2)}$  and  $Y^{(2)}$  in spin and coordinate space, respectively. Clearly, only the term

$$\Sigma_{3/2+m_{s_3}}^{(2)} Y_{-3/2-m_{s_3}}^{(2)} \quad (16)$$

of this scalar product contributes, when these operators have the magnetic-field direction as a quantization axis. The  $z$  axis normal to the surface being the natural quantization axis for the spatial part of the problem, we express the  $Y^{(2)}$  operator in terms of  $Y^{(2)}$  operators with respect to the  $z$  axis. Choosing  $x$  along the projection of  $\mathbf{B}$  as in Fig. 1, the coefficients in this expression are reduced Wigner functions

$$d_{-3/2-m_{s_3}, \mu}^{(2)}(\theta). \quad (17)$$

Here,  $\theta$  is the angle between  $\mathbf{B}$  and the surface normal and  $\mu\hbar$  is the transfer of angular momentum from the spin system to the orbital system along the  $z$  axis. The Wigner functions describe the field-orientation dependence of the amplitude. Furthermore, the  $P_Z$  dependence of  $f$  is concentrated in the exponential  $\exp(-iP_Z Z/\hbar)$  and in  $q_f$  by means of the energy-conservation relation

$$\begin{aligned} 3\epsilon_0 + \frac{p_i^2}{m_H} + \frac{3q_f^2}{4m_H} &= \frac{P_Z^2}{6m_H} + \frac{3q_f^2}{4m_H} + E_{vj} \\ &+ (\frac{3}{2} + m_{s_3})2\mu_B B, \end{aligned} \quad (18)$$

where  $E_{vj}$  is the energy of the molecular state. In the first

instance we neglect the  $P_Z^2/6m_H$  term, i.e., a possible energy transfer to the center of mass in the final state. In Sec. V we discuss also the effect of this approximation. This reduces the  $Z$  integral in Eq. (15) to a simpler Fourier integral:

$$\begin{aligned} f &= G(\mathbf{k}'_{12}, \mathbf{k}'_{13}) \\ &\times \sum_{\mu} d_{-3/2-m_{s_3}, \mu}^{(2)}(\theta) (i)^{\mu-m} e^{i(\mu-m)\phi_q} \\ &\times \int_{-\infty}^{\infty} dZ e^{-iP_Z Z/\hbar} F_{m\mu}(\theta_q, Z), \end{aligned} \quad (19)$$

where  $(\theta_q, \phi_q)$  are the polar angles of the final momentum  $\mathbf{q}_f$ . Evaluating the two integrals over the azimuthal angles  $\phi_{12}$  and  $\phi_{13}$ , reduces the expression for  $F_{m\mu}(\theta_q, Z)$  to a multiple integral over  $\rho_{12}$ ,  $z_{12}$ ,  $\rho_{13}$ , and  $z_{13}$ . This is worked out in the Appendix. There we also give the expression for  $G$  in terms of the functions  $g(k'_{12})$ ,  $g(k'_{13})$ , and  $g(|-\mathbf{k}'_{12} - \mathbf{k}'_{13}|)$ , defined in Eq. (12). In the volume case, we would obtain two separable integrals over  $r_{12}$  and  $r_{13}$ . Now the  $r_{12}$  and  $r_{13}$  integrals are not completely separable because of the surface bound states in Eq. (15). The problem, however, is still manageable numerically.

We now turn to the calculation of the rate constants  $L_s^{\pm 1/2}$ . By Parseval's theorem the integral over  $P_Z$  in Eq. (5) can be carried out analytically. Apparently, this is due to the present neglect of the  $P_Z^2/6m_H$  term in Eq. (18). As we are only interested in low temperatures, the energy pertaining to the initial state is much smaller than that of the final state. Therefore, we neglect energy changes in the final state due to the thermal-averaging procedure. With the help of Eq. (12) it is now possible to determine the temperature-dependent factor of the rate constants  $L_s^{\pm 1/2}$ .

$$\begin{aligned} \langle G^2 \rangle_T &= \langle G^2(\mathbf{k}'_{12}, \mathbf{k}'_{13}) \rangle_{\text{th}} \\ &= \frac{3}{16\pi^4} \lambda_{\text{th}}^4 \int d\mathbf{k}'_{12} \int d\mathbf{k}'_{13} \exp[-(k'_{12}{}^2 + k'_{13}{}^2 + \mathbf{k}'_{12} \cdot \mathbf{k}'_{13}) \hbar^2 / m_H k_B T] G^2(\mathbf{k}'_{12}, \mathbf{k}'_{13}) . \end{aligned} \quad (20)$$

We end up with  $L_s^{\pm 1/2}$  as a function of  $\mathbf{B}$  and  $T$ :

$$L_s^{\pm 1/2}(\mathbf{B}, T) = l_s^{\pm 1/2}(\mathbf{B}) \langle G^2 \rangle_T , \quad (21)$$

where

$$l_s^{\pm 1/2}(\mathbf{B}) = (2\pi\hbar)^8 \sum_{v,j} \frac{2\pi q_f}{4m_H} \sum_{m\mu} \int_{-\infty}^{\infty} dZ \int_{-1}^1 d(\cos\theta_q) |F_{m\mu}(\theta_q, Z)|^2 [d_{-3/2 \mp 1/2, \mu}^{(2)}(\theta)]^2 . \quad (22)$$

To exhibit more clearly the dependence on field orientation, we expand  $L_s^{\pm 1/2}$  in Legendre polynomials  $P_n(\cos\theta)$ , making use of Wigner  $3j$  symbols:

$$[d_{\sigma, \mu}^{(2)}(\theta)]^2 = \sum_n (2n+1) \begin{pmatrix} 2 & 2 & n \\ \sigma & -\sigma & 0 \end{pmatrix} \begin{pmatrix} 2 & 2 & n \\ \mu & -\mu & 0 \end{pmatrix} P_n(\cos\theta) . \quad (23)$$

The result is

$$L_s^{\pm 1/2}(\mathbf{B}, T) = \sum_{n=0,2,4} A_n^{\pm 1/2}(B, T) P_n(\cos\theta) . \quad (24)$$

Only even  $n$  values contribute because  $F_{m\mu}$  turns out to be even in  $\mu$ . Apparently, as in the volume case the double-spin-flip ( $m_{s_3} = \frac{1}{2}$ ) and single-spin-flip ( $m_{s_3} = -\frac{1}{2}$ ) contributions are related by

$$\begin{aligned} A_n^{+1/2}(B, T) \begin{pmatrix} 2 & 2 & n \\ -1 & 1 & 0 \end{pmatrix} \\ = 4 A_n^{-1/2}(2B, T) \begin{pmatrix} 2 & 2 & n \\ -2 & 2 & 0 \end{pmatrix} , \end{aligned} \quad (25)$$

where the factor of 4 results from the spin-matrix element of Eq. (15). Equation (25) is the counterpart of a similar relation between  $L_g^{+1/2}$  and  $L_g^{-1/2}$  for the volume.

### III. RESULTS

As in the volume case, the most important molecular states appear to be the states close to the continuum. For fields below 10 T 99% of the total contribution to the effective rates comes from the  $v=14, j=3$  state, with a binding energy of 72 K, and the small remaining fraction from the  $v=14, j=1$  state, with a binding energy of 183 K. This fraction becomes the dominant part for higher fields.

In the previous section we used the wave function  $\phi_0(z)$  of Mantz and Edwards<sup>21</sup> to calculate the effective potentials  $V^{\text{eff}}$  of Eq. (9). To keep computation time within reasonable bounds, we prefer to use the form  $\phi_0(z) = 2\alpha^{3/2} z \exp(-\alpha z)$  for calculating  $f$ . For  $\alpha = 0.15a_0^{-1}$ ,  $\phi_0$  resembles rather closely the Mantz and Edwards wave function, while for  $\alpha = 0.20a_0^{-1}$  it resembles the wave function in a Stwalley-type potential<sup>8</sup> reproducing the experimental adsorption energy. In most of the calculations we shall use the former value for  $\alpha$ . The error bar in some of the results to be given corresponds with the change in  $L_s^{\text{eff}}$  as a consequence of the replacement of this value by  $\alpha = 0.20a_0^{-1}$ . It turns out that our values for  $L_s^{\text{eff}}$  scale roughly with  $\alpha^2$ , which would

suggest the validity of the scaling prescription<sup>15</sup> (see, however, Sec. IV).

In Fig. 2 we present the partial contributions  $A_n^{-1/2}$  ( $n=0,2$ ) to  $L_s^{\text{eff}}$  as a function of  $B$  at  $T=0.4$  K (dashed curves). We also present the partial effective rate constants  $A_n^{-1/2} + 2A_n^{+1/2}$  for  $n=0,2$  (solid curves). Note that in I we presented values for  $L_s$  instead of  $L_s^{\text{eff}}$ . The remaining differences between the results of I and Fig. 2 can be explained by the fact that we here use a H-H potential, which reproduces more accurately the experimental data on singlet boundstate energies. Therefore the effective potentials of Eq. (9) and the wave functions  $u_{vjm}$  and  $v^t$  are slightly changed. An important effect comes from the increase of the binding energy of the  $v=14, j=3$  state by about 6 K, which results in a shift of the curves of the rate constant as a function of  $B$ . From Fig. 2 we may conclude that the anisotropy is small, which is caused by the fact that all  $\mu$  values in Eq. (22) give contributions of the same order of magnitude. This seems to be in agreement with experimental indications.<sup>12,22</sup>

Both the field dependence and absolute magnitude of the effective rate constant, however, are at variance with experiment. We find a rate which is growing with  $B$  by 70% from  $B=4$  to 9 T, whereas experiments show a slow decrease. For the field orientation normal to the surface we find  $L_s^{\text{eff}} = 2.7(7) \times 10^{-25} \text{ cm}^4 \text{ s}^{-1}$  at  $B=7.6$  T and  $T=0.4$  K, while the corresponding experimental values are  $L_s^{\text{eff}} = 1.5(2) \times 10^{-24} \text{ cm}^4 \text{ s}^{-1}$  (Ref. 22) and  $L_s^{\text{eff}} = 1.8(4) \times 10^{-24} \text{ cm}^4 \text{ s}^{-1}$  (Ref. 12). These values are a factor of 6 larger than our calculated value. In Ref. 15 it was noticed that a scaling prescription to convert the volume rate into a surface rate, leads to a correct order of magnitude for  $L_s^{\text{eff}}$ . (More precisely, the difference with experiment is a factor of 2.) Objections against this scaling prescription will be presented in the following section.

In Fig. 3 we present the temperature dependence of the rate, governed by the function  $\langle G^2 \rangle_T$  of Eq. (20). As a reference temperature we use  $T_0=0.4$  K and therefore we plotted  $\langle G^2 \rangle_T / \langle G^2 \rangle_{T_0}$  as a function of  $Y$ . Note that  $L_s^{\text{eff}}$  goes to zero logarithmically for  $T \rightarrow 0$ , illustrating again that a zero-temperature approximation as in three

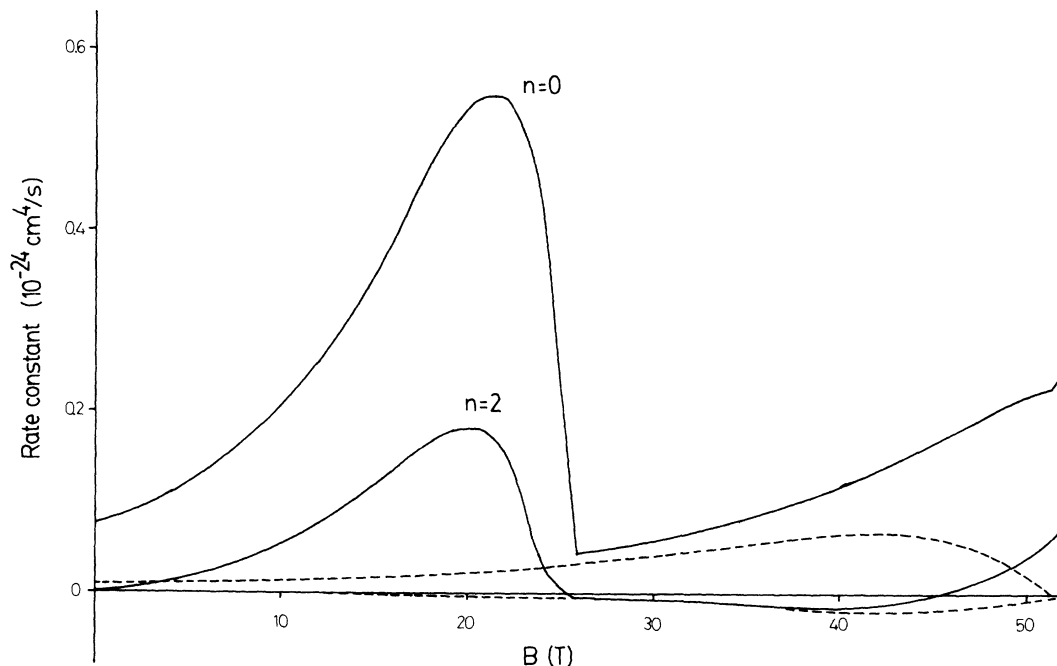


FIG. 2. Partial contributions to  $L_s^{\text{eff}}$  as a function of  $B$  ( $T=0.4$  K,  $\alpha=0.15a_0^{-1}$ ). Dashed curves: single-spin-flip fractions  $A_n^{-1/2}$ . Solid curves: effective rate constant  $A_n^{-1/2} + 2A_n^{+1/2}$ .

dimensions is not feasible.

As can be seen from Eq. (22),  $L_s^{\pm 1/2}$  is essentially an incoherent sum (integral) over  $m$ ,  $\mu$ ,  $Z$ , and  $\theta_q$  of  $|F_{m\mu}(Z, \theta_q)|^2$ . To understand the underlying physics, we plot in Fig. 4 the  $|F_{m\mu}(Z, \theta_q)|^2$  surfaces as a function of  $Z$  and  $\theta_q$  for various  $|\mu|, |m|$  combinations ( $B=7.6$  T,  $\alpha=0.5 a_0^{-1}$ ,  $v=14$ ,  $j=3$ ,  $m_{s_3}=-\frac{1}{2}$ ). In Fig. 4 the maximum value of the  $m=\mu=0$  surface has arbitrarily been

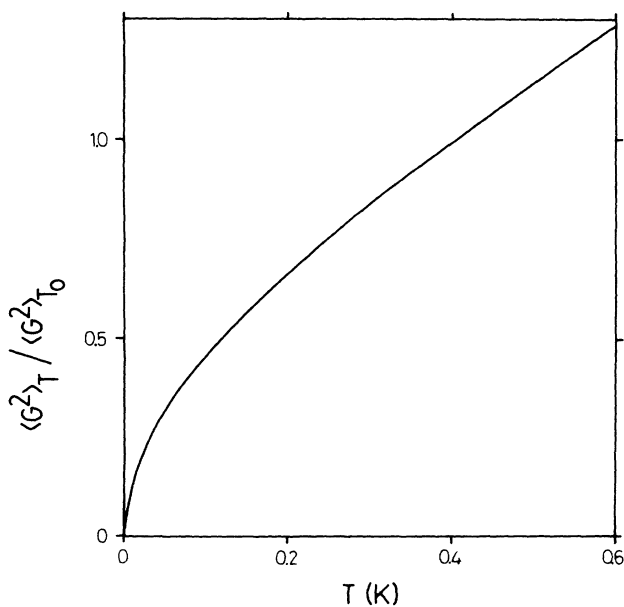


FIG. 3. The function  $\langle G^2 \rangle_T / \langle G^2 \rangle_{T_0}$  as a function of  $T$  for  $T_0=0.4$  K.

taken as 1. All surfaces have their maximum value for  $Z \simeq 7a_0$ , which corresponds to the most probable location of the atoms from the wall in the  $\phi_0$  state. For  $\sin\theta_q \rightarrow 1$  the dominant  $|F|^2$  surfaces show a decrease which is due to the absence of high relative momenta along the surface in the initial state. A similar feature gives rise to the increase of  $L_s^{\text{eff}}$  with  $B$  at lower fields. The absence of high initial momenta along the surface is also responsible for the gradual shift of the maximum of the  $|F|^2$  surface to larger  $\sin\theta_q$  values for increasing  $|m|$  and  $|\mu|$ : atom 3 can only gain high momentum  $q_{\parallel}$  by the dipole interaction, say with atom 1. The strong  $xy$  recoil of atom 1, however, enhances rapid rotation (large  $|m|$ ) of atom 1 and 2, which has not been involved in the dipole force. On the other hand, strong dipole forces along the surface are correlated with high transfers  $|\mu|$  of  $z$ -angular momentum from the spin system to the spatial degrees of freedom. The above picture also explains that the absolute value of the surfaces decreases for increasing  $|m|$  and  $|\mu|$ . Via Eq. (22) this would seem to be inconsistent with the previously mentioned small anisotropy as a function of  $\theta$ . It turns out, however, that the solid angle in which atom 3 is emitted decreases for decreasing  $|\mu|$ . This leads to comparable contributions of all  $|\mu|$  values and thus a nonsignificant anisotropy of the rate constant with respect to the magnetic field direction. It turns out that the summation over  $\mu$  also washes out the anisotropic structure as a function of  $\sin\theta_q$  implied by the individual surfaces in Fig. 4.

#### IV. SCALING PRESCRIPTION

As has been pointed out in the previous section, the scaling procedure, proposed by Kagan *et al.*<sup>15</sup> leads to

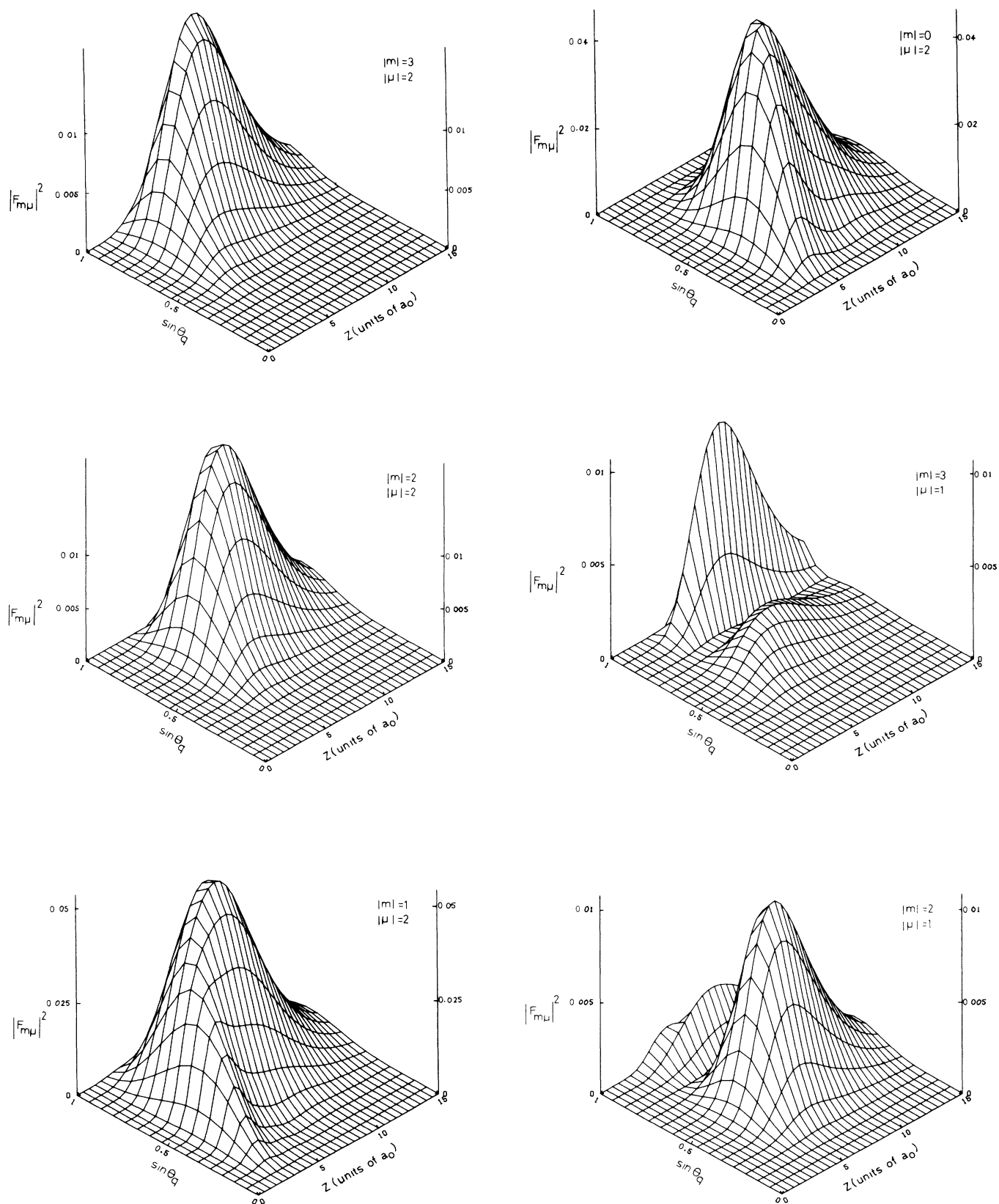


FIG. 4. Transition probability  $|F_{m\mu}(Z, \theta_q)|^2$  as a function of  $Z$  and  $\sin\theta_q$  for all  $|m|$  (rotational angular momentum) and  $|\mu|$  (angular momentum transfer) values. ( $B=7.6$  T,  $\alpha=0.15a_0^{-1}$ ,  $v=14$ ,  $j=3$ ,  $m_{j3}=-\frac{1}{2}$ ). All surfaces are normalized relative to the maximum of the  $m=\mu=0$  surface.

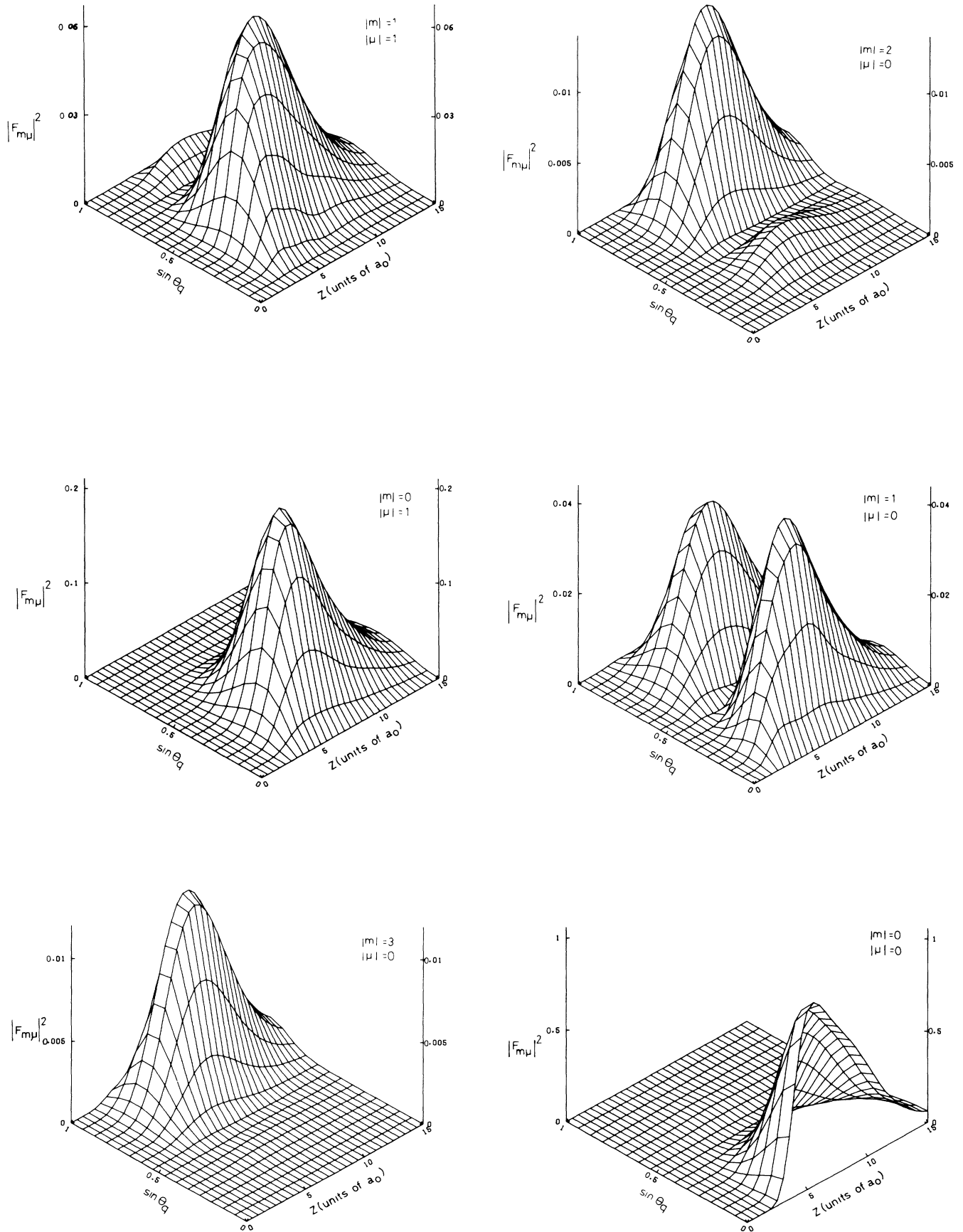


FIG. 4. (Continued).

surface rates which differ by more than an order of magnitude from the values presented here. Their results agree better with the experimental data. We believe, however, that this scaling procedure is a bad approximation in the present situation. To show this, let us analyze step by step where the above-mentioned large difference with our  $L_s^{\text{eff}}$  value arises from.

In Ref. 15 Kagan *et al.* claim that a state of adsorbed atoms can be regarded as quasi-three-dimensional, when the width of the one-atom  $z$  wavefunction is much larger than the interaction range of the particles. (In the case of polarized atomic hydrogen atoms the interaction range  $r_0 \simeq 6a_0$  and the  $^4\text{He-H}$  potential well has a width of  $d \simeq 10a_0 - 20a_0$ .) The initial state is considered to be a product of a 3D relative three-atom state and three surface bound states  $\tilde{\phi}_0$ . The authors use the function  $\tilde{\phi}_0(z) = (2\tilde{\alpha})^{1/2} \exp(-\tilde{\alpha}z)$ , with  $\tilde{\alpha} = \sqrt{2m_H|\epsilon_0|}/\hbar$ , as a bound state. A choice of 0.9 K for  $|\epsilon_0|$  in the case of a  $^4\text{He}$  film leads to a value of  $0.10a_0^{-1}$  for  $\tilde{\alpha}$ . Strictly speaking, the exponential form is only assumed for large positive  $z$ . The normalization factor implies a cutoff close to  $z=0$ . The simple exponential form introduces a simplification in that the product of bound states then depends only on  $Z$ . When the relative and center-of-mass motion are subsequently treated independently, this leads to a very simple relation between the surface and bulk rates

$$\tilde{L}_s^{\text{eff}} = \frac{4}{3} \tilde{\alpha}^2 L_g^{\text{eff}}. \quad (26)$$

At a field of 7.6 T, where the Kagan dipole rate constant has the value  $L_g^{\text{eff}} = 6.8 \times 10^{-39} \text{ cm}^6 \text{ s}^{-1}$ , this leads to  $\tilde{L}_s^{\text{eff}} = 3.2 \times 10^{-24} \text{ cm}^4 \text{ s}^{-1}$  for the surface rate constant, which is a factor of 16 larger than our value  $L_s^{\text{eff}} = 2.0 \times 10^{-25} \text{ cm}^4 \text{ s}^{-1}$  for  $B = 7.6 \text{ T}$ ,  $\theta = 0$ ,  $T = 0.4 \text{ K}$ ,  $\alpha = 0.15a_0^{-1}$  (and only a factor of 2 different from experiment).

We notice that the bound states  $\phi_0$  and  $\tilde{\phi}_0$  of the two models are different. The widths  $\Delta z$  of the wavefunctions are comparable, however. To analyze the differences between the two models, we first try to find out how the result of our calculation is modified by replacing our  $\phi_0$  and  $\alpha$  by  $\tilde{\phi}_0$  and  $\tilde{\alpha}$ . This leads to an increase of  $L_s^{\text{eff}}$  by a factor 2.4, which indicates that the different choice of bound states is not the main reason for the large difference.

In the derivation of Eq. (26) by Kagan *et al.*, the relative and center-of-mass motions are considered to be independent, which is not strictly justified, since all three-particle coordinates perpendicular to the surface should essentially be positive. This gives rise to restrictions in relative  $z$  coordinates, which have been taken into ac-

count correctly in our model, but not in the scaling procedure. If we introduce the same approximation in our calculation, this leads to another increase by a factor of 1.6. The remaining factor of 4.2 can only be accounted for by the two- and three-dimensional natures of the relative three-atom state, used in the two models.

As we already pointed out, Kagan *et al.* argue that the nature of this state should be three-dimensional when  $d \gg r_0$ . However, a third length scale plays a crucial role: the wavelength  $\lambda$ . For  $d \gg \lambda$  the well would indeed be wide enough to justify this approximation, especially near the interaction region. However, the actual situation is closer to the opposite limit: At 0.4 K the wavelength  $\lambda \simeq 130a_0$ . In this situation the typical single-particle energy separation  $|\epsilon_0| = \hbar^2/(2m_H d^2)$  in the  $z$  direction is larger than the relative kinetic energy  $4\pi^2\hbar^2/(m_H\lambda^2)$  along the surface, thus impeding transitions in which the  $z$  eigenstate  $\phi_0$  is changed. Freezing the  $\phi_0$  eigenstate in the  $z$  direction, however, is the basic assumption leading to the  $2\frac{1}{2}D$  mode. A  $2\frac{1}{2}D$  approach therefore seems more appropriate than the limiting situation  $|\epsilon_0| \ll 4\pi^2\hbar^2/(m_H\lambda^2)$  in which the atoms would behave unconfined also in the  $z$  direction. This is also the main conclusion reached in previous more exact calculations<sup>8,9</sup> of  $b + b$  surface dipole relaxation.

To make the comparison of our surface recombination model with the scaling approach complete, we also replaced our 2D triplet functions in Eq. (15) by 3D ones. This indeed resolved the last factor of 4.2 discrepancy. It is of interest here to point to the radically different low-energy behaviors of 2D and 3D relative two-particle wave functions: 2D wave functions tend to zero logarithmically, as can be seen from Eq. (12), while 3D wave functions are finite in this limit. This feature expresses itself in the temperature dependence of  $\langle G^2 \rangle_T$  (see Fig. 3) and thus represents a characteristic difference with the scaling result.

## V. DISCUSSION OF SOME APPROXIMATIONS

In this section we estimate the errors introduced by some of the approximations in the previous sections. To begin with, we neglected the center-of-mass energy in the final state in Eq. (18). If we take it into account, it leads to a redistribution of the energy released by the recombination among the relative atom-molecule motion and the center-of-mass motion in the final state. As a result, we cannot use Parseval's theorem to simplify the calculation, but we have to use Eqs. (5) and (6) to calculate  $L_s^{\pm 1/2}$  and  $f$ . All equations presented in Sec. II remain valid, except for Eq. (22), which has to be replaced by

$$L_s^{\pm 1/2}(\mathbf{B}) = (2\pi\hbar)^8 \sum_{v,j} \frac{2\pi}{4m_H} \sum_{m,\mu} \int_{-\infty}^{\infty} dP_Z q_f(P_Z) \int_{-1}^1 d(\cos\theta_q) \left| \int_{-\infty}^{\infty} dZ \frac{e^{-iP_Z Z/\hbar}}{(2\pi\hbar)^{1/2}} F_{m\mu}(\theta_q, Z) \right|^2 [d_{-3/2 \mp 1/2, \mu}^{(2)}(\theta)]^2 \quad (27)$$

keeping in mind that  $F_{m\mu}$  also depends on  $P_Z$  through its dependence on  $q_f(P_Z)$ . Since the center of mass now absorbs part of the recombination energy, the average value of  $q_f$  decreases compared to the situation before. Therefore the curve of the rate constant as a function of  $B$ ,

presented in Fig. 2, is expected to shift to lower field values. For  $B = 7.6 \text{ T}$ ,  $T = 0.4 \text{ K}$  and field orientation perpendicular to the surface we now find  $L_s^{\text{eff}} = 2.2 \times 10^{-25} \text{ cm}^4 \text{ s}^{-1}$ , which is a factor of 1.1 larger than the corresponding value given in Sec. III. In Fig. 5 we

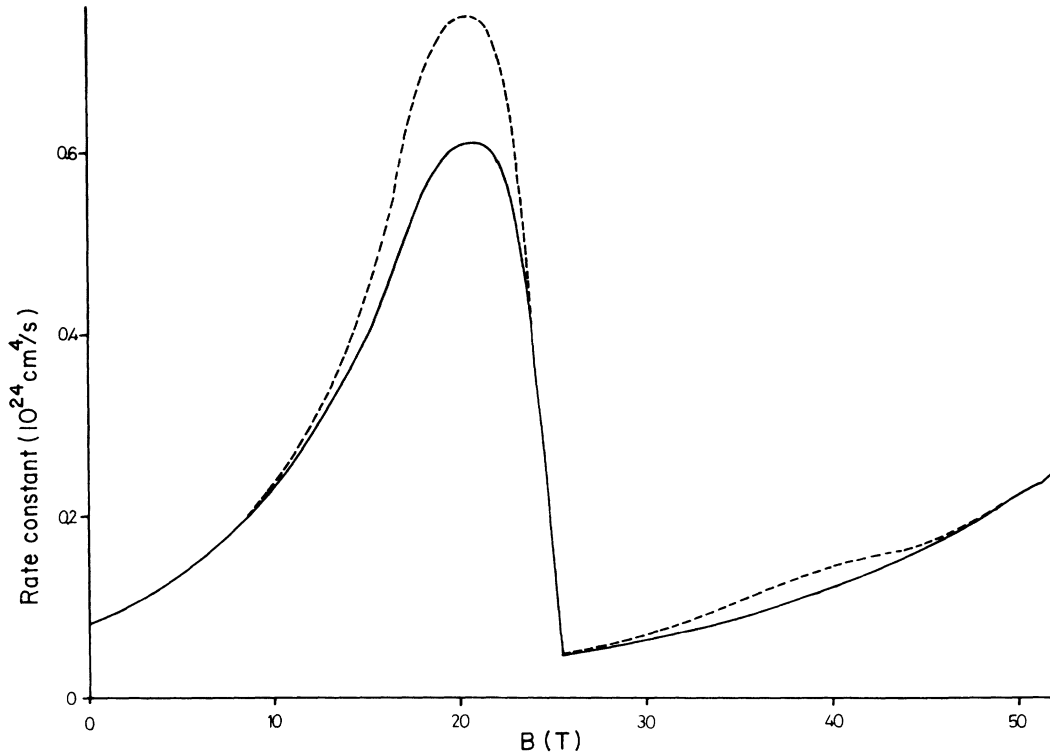


FIG. 5. The field dependence of the effective rate constant averaged over field directions: (1) solid curve, without wall, but center-of-mass energy in the  $z$  direction taken into account; (2) dashed curve, with rigid wall.

present the effective rate constants averaged over field orientations as a function of  $B$  (solid curve). Altogether we find a shift of the curve by about 1.5 T, which corresponds to an average of 2.0 K for  $P_z^2/6m_H$ . This is at least a factor of 20 smaller than the average kinetic energy  $3q_f^2/4m_H$ . The expectation value of the kinetic energy  $P_z^2/6m_H$  in the initial state  $\phi_0(z_1)\phi_0(z_2)\phi_0(z_3)$  is  $\hbar^2\alpha^2/2m_H$  for the analytic choice of our bound state. This leads to a value of 2.0 K for the center-of-mass energy if  $\alpha=0.15a_0^{-1}$  and is in agreement with the shift found here. Furthermore, the field dependence of  $L_s^{\text{eff}}$  as a function of  $B$  found in Sec. III is hardly changed. The smallness of the effect is related to the small expectation value and spread in the center-of-mass energy compared to the relative kinetic energy.

The derivation of  $L_s$  and  $f$ , given in Ref. 16, leads to expressions for these quantities in which the influence of the inert wall is included in the final state  $\psi^{(-)}$ . In Sec. II, however, the actual calculation was carried out without it. This might seem a very crude approximation, because the atom-wall interaction has a strong repulsive part for small distances. Therefore, we will now estimate the effect of this approximation. We improve the model described in Sec. II by assuming that the surface is a hard rigid wall. As we already explained, the shallow attractive part of the surface potential is neglected for the final state (but not for the initial state). The atom and molecule are now offered the possibility to reflect from this wall in the final state. In principle the molecule could be deexcited to states with higher binding energy by these collisions. This is not likely, however, because the addi-

tional energy released would give rise to higher final momenta, and a decreasing overlap with the initial state. Therefore we will only consider reflections of the center of mass of the molecule from the surface.

To compare with the case without a wall, we explicitly give the expressions for both models here. Without wall Eq. (5) can be rewritten as

$$L_s^{\pm 1/2} = (2\pi\hbar)^7 \frac{1}{4m_H} \sum_n \sum_\alpha \int d\varphi_q \int dp_{\text{at},z} \int dp_{\text{mol},z} \times \langle |f_{q_f P_z n \pm 1/2, p_i q_i \alpha}|^2 \rangle_{\text{thermal}}, \quad (28)$$

where the momenta perpendicular to the surface

$$P_{\text{at},z} = \frac{1}{3}P_z + q_z, \quad p_{\text{mol},z} = \frac{2}{3}P_z - q_z \quad (29)$$

can be both positive and negative. The final-state vector  $|\psi^{(-)}(q_f P_z n \pm \frac{1}{2})\rangle$  in Eq. (6) for  $f_{q_f P_z n \pm 1/2, p_i q_i}$  is then given by Eq. (14), where the  $z$  motion is described by

$$|p_{\text{at},z}, p_{\text{mol},z}\rangle \triangleq \frac{e^{ip_{\text{at},z}z_3/\hbar}}{(2\pi\hbar)^{1/2}} \frac{e^{ip_{\text{mol},z}(z_1+z_2)/2\hbar}}{(2\pi\hbar)^{1/2}}. \quad (30)$$

In the case including the wall the integrals over  $p_{\text{at},z}$  and  $p_{\text{mol},z}$  in Eq. (28) run from 0 to  $\infty$ , because the particles can only move away from the surface. Furthermore, the plane-wave part Eq. (30) should be supplemented with "time-reversed" reflected waves of atom and molecule:

$$\begin{aligned} & |p_{\text{at},z}, p_{\text{mol},z}\rangle + |-p_{\text{at},z}, -p_{\text{mol},z}\rangle, \\ & -|p_{\text{at},z}, -p_{\text{mol},z}\rangle - |-p_{\text{at},z}, p_{\text{mol},z}\rangle. \end{aligned} \quad (31)$$

For the following it is of importance to point out that we may now extend the ranges of integration of  $p_{\text{at},z}$  and  $p_{\text{mol},z}$  again to  $(-\infty, \infty)$  if we multiply Eq. (28) by an additional factor  $\frac{1}{4}$ . The total  $z$  wave function now vanishes for  $z_3=0$  and for  $\frac{1}{2}(z_1+z_2)=0$ . We note that the integrals over  $z_3$  and  $\frac{1}{2}(z_1+z_2)$  in the expression for the amplitude  $F$  run over positive values only.

We were able to calculate the rate constant numerically for this case of a rigid wall. In Fig. 5 we plot the effective rate constant averaged over magnetic-field directions as a function of  $B$  at  $T=0.4$  K for the case including the wall (broken curve). We see that the difference with the case without a wall is not significant. It is at most 20%. There is also no sign of change with respect to the field-orientation dependence. The similarity between these results can be explained as follows. In good approximation the four terms of Eq. (31) give rise to equal and noninterfering contributions to the transition probability, which add up to the original result. As a matter of fact, the main contribution of the terms comes from nonoverlapping parts of the  $(p_{\text{at},z}, p_{\text{mol},z})$  plane. As has been pointed out in the foregoing, small center-of-mass momenta in the  $z$  direction are dominant. Therefore the dominant regions in the  $(p_{\text{at},z}, p_{\text{mol},z})$  plane are the parts where  $p_{\text{at},z} \approx -p_{\text{mol},z}$  ( $p_{\text{at},z} > 0$ ),  $p_{\text{at},z} \approx -p_{\text{mol},z}$  ( $p_{\text{at},z} < 0$ ),  $p_{\text{at},z} \approx p_{\text{mol},z}$  ( $p_{\text{at},z} > 0$ ), and  $p_{\text{at},z} \approx p_{\text{mol},z}$  ( $p_{\text{at},z} < 0$ ) for the terms of Eq. (31), respectively. Because of the absence of high momenta along the surface,  $p_{\text{at},z}^2/2m_H + p_{\text{mol},z}^2/4m_H$  is large for weaker fields. Consequently, the foregoing regions do not overlap and do not interfere. For stronger fields this is no longer the case and the difference with the results without a wall is indeed observed to increase.

## VI. CONCLUSION

In the foregoing we described a method, based on the Kagan dipole mechanism, for the calculation of the three-body dipolar recombination rate for atoms adsorbed on a  $^4\text{He}$  film. The results can be summarized as follows. (1) At a field of 7.6 T and temperature of 0.4 K we obtained  $L_s^{\text{eff}} = 2.7(7) \times 10^{-25} \text{ cm}^4 \text{ s}^{-1}$ , which is about a factor of 6 smaller than the experimental value. (2) The field-orientation dependence of the effective rate constant is found to be weak, which agrees with experimental data. (3) We predict a strong increase of  $L_s^{\text{eff}}$  with increasing temperature between  $T=0.1$  and 0.6 K. It might be interesting to include this in the analysis of the experi-

ments. (4) The field dependence of  $L_g^{\text{eff}}$  calculated by Kagan *et al.*<sup>3</sup> and that of  $L_s^{\text{eff}}$  display a similar behavior and disagree both with the experimental  $B$  dependence.

Although the model we presented here is far from exact, we believe that the essential features of the interaction of the particles with the wall are included. Some refinements to improve the model in connection with the influence of the inert wall have shown to be of minor importance. Part of this discrepancy with the experimental data may be ascribed to the dynamical role of the wall. However, since the magnetic-field dependence of the volume and surface rate constants display similar deviations, it is likely that the discrepancies in both cases are caused by the same mechanism. We have strong indications that the discrepancy in the volume case is caused by the neglect of interactions between the final-state molecule and atom, in particular by the absence of exchange: A more rigorous calculation of volume recombination, in which all three-particle correlations are included except for exchange, lowers the rate constants to values a factor of 5 too small compared to the experimental data.<sup>23</sup> The physical picture underlying this correlation effect is the quenching of the dipole force at small distances due to repulsion. From the same physical picture we expect the above-mentioned factor of 6 surface discrepancy to show a further increase, when similar correlations would be taken into account. It seems probable that the dipole-exchange mechanism<sup>18</sup> is crucial to resolve the discrepancies for both volume and surface recombination. It remains to be seen, however, whether a calculation including this mechanism would be feasible in the surface case, where a great part of the symmetry of the volume is lost.

## ACKNOWLEDGMENT

This work is part of a research program of the ‘‘Stichting voor Fundamenteel Onderzoek der Materie’’ (FOM) which is financially supported by the ‘‘Nederlandse Organisatie voor Zuiver Wetenschappelijk Onderzoek’’ (ZWO).

## APPENDIX

We here present a complete expression for the reduced amplitude  $F_{m\mu}(\theta_q, \mathbf{Z})$  of Eq. (19) for fixed final-state quantum numbers  $v, j, m, m_s, q_f$  and fixed  $\mu, \mathbf{Z}$ :

$$F_{m\mu}(\theta_q, \mathbf{Z}) = \frac{\frac{2}{3}m_H}{2\pi\hbar^2} \frac{2\delta_{j,\text{odd}}}{(2\pi\hbar)^2} (2\pi)^2 \frac{\mu_0\mu_B^2}{4\pi} \left[ \frac{12\pi}{5} \right]^{1/2} (1 - 3\delta_{m_s, 1/2}) \\ \times \int_{-3Z}^{3Z} dz_{12} e^{-iq_z z_{12}/2\hbar} \int_a^b dz_{13} e^{+iq_z z_{13}/\hbar} I_m(z_{12}, q_{\parallel}) K_{\mu}(z_{13}, q_{\parallel}) \phi_0(z_1) \phi_0(z_2) \phi_0(z_3). \quad (\text{A1})$$

This includes the subsidiary conditions  $z_i \geq 0$  introduced in Sec. IV, which also lead to

$$a = \min(-3Z - z_{12}, -3Z + 2z_{12}), \\ b = \frac{3}{2}Z + \frac{1}{2}z_{12}. \quad (\text{A2})$$

Furthermore,

$$I_m(z_{12}, q_{\parallel}) = \int_0^{\infty} d\rho_{12} \rho_{12} \hat{v}^i(\rho_{12}) J_m(q_{\parallel} \rho_{12} / 2\hbar) \frac{u_{vj}(r_{12})}{r_{12}} Y_{jm}(\theta_{12}, 0), \quad (\text{A3})$$

$$K_{\mu}(z_{13}, q_{\parallel}) = \int_0^{\infty} d\rho_{13} \rho_{13} \hat{v}^i(\rho_{13}) J_{\mu}(q_{\parallel} \rho_{13} / \hbar) \frac{(Y_{2\mu}(\theta_{13}, 0))}{r_{13}^3},$$

represent the uncoupled integrals along the surface with  $q_{\parallel} = q_f \sin \theta_q$  and  $q_z = q_f \cos \theta_q$ . The functions  $J_m$  are cylindrical Bessel functions and  $\cos \theta_{ij} = z_{ij} / r_{ij}$ . Finally, the energy dependence in the  $f$  amplitude is concentrated in the function

$$G(\mathbf{k}'_{12}, \mathbf{k}'_{13}) = 2[g(k'_{12})g(k'_{13}) + g(k'_{13})g(|-\mathbf{k}'_{12} - \mathbf{k}'_{13}|) + g(k'_{12})g(|-\mathbf{k}'_{12} - \mathbf{k}'_{13}|)]. \quad (\text{A4})$$

- <sup>1</sup>F. London, *Superfluids* (Dover, New York, 1961), Vol. I; *ibid.* (Wiley, New York, 1954), Vol. II.
- <sup>2</sup>T. J. Greytak and D. Kleppner, in *New Trends in Atomic Physics*, Proceedings of the Les Houches Summer School, 1982, edited by G. Greenberg and R. Stora (North-Holland, Amsterdam, 1984), p. 1125.
- <sup>3</sup>I. F. Silvera and J. T. M. Walraven, *Progress in Low Temperature Physics*, edited by D. F. Brewer (North-Holland, Amsterdam, 1985), Vol. X, p. 139.
- <sup>4</sup>B. W. Statt and A. J. Berlinsky, *Phys. Rev. Lett.* **45**, 2105 (1980).
- <sup>5</sup>A. Legendijk, *Phys. Rev. B* **25**, 2054 (1982).
- <sup>6</sup>A. E. Ruckenstein and E. D. Siggia, *Phys. Rev. B* **25**, 6031 (1982).
- <sup>7</sup>B. W. Statt, *Phys. Rev. B* **25**, 6035 (1982).
- <sup>8</sup>R. M. C. Ahn, J. P. H. W. van den Eijnde, C. J. Reuver, B. J. Verhaar, and I. F. Silvera, *Phys. Rev. B* **26**, 452 (1982).
- <sup>9</sup>J. P. H. W. van den Eijnde, C. J. Reuver, and B. J. Verhaar, *Phys. Rev. B* **28**, 6309 (1983).
- <sup>10</sup>M. Papoular, *J. Phys. B* **18**, L821 (1985).
- <sup>11</sup>Yu. Kagan, I. A. Vartan'yants, and G. V. Shlyapnikov, *Zh. Eksp. Teor. Fiz.* **81**, 1113 (1981) [*Sov. Phys.—JETP* **54**, 590 (1981)].
- <sup>12</sup>H. F. Hess, D. A. Bell, G. P. Kochanski, D. Kleppner, and T. J. Greytak, *Phys. Rev. Lett.* **52**, 1520 (1984).
- <sup>13</sup>M. W. Reynolds, I. Shinkoda, W. N. Hardy, A. J. Berlinsky, F. Bridges, and B. W. Statt, *Phys. Rev. B* **31**, 7503 (1985); B. W. Statt, W. N. Hardy, A. J. Berlinsky, and E. Klein, *J. Low Temp. Phys.* **61**, 471 (1985); B. W. Statt, A. J. Berlinsky, and W. N. Hardy, *Phys. Rev. B* **31**, 3169 (1985).
- <sup>14</sup>L. P. H. de Goey, J. P. J. Driessen, B. J. Verhaar, and J. T. M. Walraven, *Phys. Rev. Lett.* **53**, 1919 (1984).
- <sup>15</sup>Yu. Kagan, G. V. Shlyapnikov, I. A. Vartan'yants, and N. A. Glukhov, *Zh. Eksp. Teor. Fiz.* **81**, 1131 (1981) [*Sov. Phys.—JETP* **35**, 477 (1982)].
- <sup>16</sup>L. P. H. de Goey, Ph.D. thesis, Eindhoven University of Technology, 1988.
- <sup>17</sup>W. Glöckle, *The Quantum Mechanical Few-Body Problem*, (Springer-Verlag, Berlin, 1983).
- <sup>18</sup>L. P. H. de Goey, T. H. M. v.d. Berg, N. Mulders, H. T. C. Stoof, B. J. Verhaar, and W. Glöckle, *Phys. Rev. B* **34**, 6183 (1986).
- <sup>19</sup>L. D. Faddeev, *Zh. Eksp. Teor. Fiz.* **39**, 1459 (1961) [*Sov. Phys.—JETP* **12**, 1014 (1961)].
- <sup>20</sup>B. J. Verhaar, J. P. H. W. van den Eijnde, M. A. J. Voermans, and M. M. J. Schaffrath, *J. Phys. A* **17**, 595 (1984); J. P. H. W. van den Eijnde, Ph.D. thesis, Eindhoven University of Technology, 1984; B. J. Verhaar, L. P. H. de Goey, J. P. H. W. van den Eijnde, and E. J. D. Vredendregt, *Phys. Rev. A* **32**, 1424 (1985); **32**, 1430 (1985); B. J. Verhaar, L. P. H. de Goey, E. J. D. Vredendregt, and J. P. H. W. van den Eijnde, *Phys. Lett.* **110A**, 371 (1985).
- <sup>21</sup>I. B. Mantz and D. O. Edwards, *Phys. Rev. B* **20**, 4518 (1979).
- <sup>22</sup>R. Sprik, J. T. M. Walraven, G. H. v. Yperen, and I. F. Silvera, *Phys. Rev. B* **34**, 6172 (1986).
- <sup>23</sup>L. P. H. de Goey, H. T. C. Stoof, B. J. Verhaar, and W. Glöckle, *Phys. Rev. B* **38**, 646 (1988).